

Oxygen over-stoichiometry in the 2H-perovskite related structure: The route to cation deficient Ising chain oxides $\text{Sr}_{1+\gamma}[(\text{Mn}_{1-x}\text{Co}_x)_{1-z}\square_z]\text{O}_3$

SUPPLEMENTAL INFORMATION

Single crystals were extracted from two synthesis batches of nominal compositions $\text{Sr}_{11/8}[\text{Mn}_{5/8}\text{Co}_{3/8}\text{O}_{3+\delta}]$ (I) and $\text{Sr}_{4/3}[\text{Mn}_{2/3}\text{Co}_{1/3}\text{O}_{3+\delta}]$ (II); the selected crystals were tested using a 4-circles single crystal diffractometer Synergy S from RIGAKU equipped with a Mo photonjet microfocus source and an Eiger 1M HPC X-ray detector from Dectris. Specimen with the highest crystalline quality were chosen for X-ray single crystal data collections. Crystals from both batches exhibit composite structures characterized by the 2 following trigonal sub-lattices:

$$a_1=a_2\sim 9.6 \text{ \AA}, b_1=b_2\sim 9.6 \text{ \AA}, c_1\sim 2.6 \text{ \AA}, c_2\sim 3.9 \text{ \AA}, \alpha=\beta=90^\circ \gamma=120^\circ \mathbf{q}_1= c_1/c_2 \mathbf{c}_1^* = \gamma_1 \mathbf{c}_1^*, \mathbf{q}_2= c_2/c_1 \mathbf{c}_2^* = \gamma_2$$

\mathbf{c}_2^* . The transformation matrix between the sub-lattice 1 and 2 is $W^2 = \begin{pmatrix} 1 & 0 & 0 & 0 \\ 0 & 1 & 0 & 0 \\ 0 & 0 & 0 & 1 \\ 0 & 0 & 1 & 0 \end{pmatrix}$. The super space group describing the symmetry of sub-lattice 1 is R-3m (00 γ_1)0s and the one of the sub-lattice 2 is X-3c1(00 γ_2)000 with X corresponding to (2/3 1/3 0 1/3 ; 1/3 2/3 0 2/3) centering vectors [1]. The general chemical formula of these 2 types of crystals is $\text{Sr}_{1+x}(\text{Mn}_{1-x}\text{Co}_x)\text{O}_{3+\delta}$. $(\text{Mn}_{1-x}\text{Co}_x)\text{O}_{3+\delta}$ part belongs to sub-lattice 1 and Sr_{1+x} to sub-lattice 2. Owing to the scattering factors of the different species in the system, the contribution of the sub-lattice 2 dominates the diffraction pattern. For this reason the sub-lattice 2 is considered as a reference sub-lattice for the determination and the refinement of the metric of the system; the use of the strongest reflections stabilizes the refinement of the cell parameters. Note that for the sake of simplification, the notation $\gamma = \gamma_1=1/\gamma_2$ is used all along the text.

Full data collections were performed on crystals of batches I and II (they will be called crystal I and crystal II respectively); cell parameters are summarized in Table SI-1. The main difference between the 2 samples is related to the value of the c_1/c_2 ratio; this is illustrated in the figure SI-1. Looking at red line, one can see the alignment of the reflections for the crystal of batch I and the deviation from the line for the reflections of the crystal of batch II. These features are related to the commensurate and incommensurate character of the structural modulations of batches I and II respectively (see the value of the components of the wave vectors in Table SI-1). The data integration in the (3+1)d approach is performed using CrysAlispro [2] but following a list of reflections generated with a jana2006 [3] sub routine considering the two subsystems and the (3+1)d superspace defined above. Such procedure prevents overlapping of integration boxes due to the generation satellite reflections with too high m index in the procedure developed for classical incommensurate modulated structure.

Due to the rational value evidenced for the modulation vector of the crystal I, two different indexations can be proposed: either with a classical supercell (cell: $a_1 b_1 3 \times c_1$) or the (3+1)d cell. Consequently, both classical method and superspace approach can be and will be used to solve the structure of the crystal I; a comparison of the results would help us to validate the analysis and to check the limitations of both technics. The crystal II is exhibiting an aperiodic structure and thus only the (3+1)d refinement leads to correct solution.

(3+1)d Structural analysis of the crystals I and II

Using the superspace approach the crystal structure of both samples is fully described from the Sr sublattice defined by a single independent strontium atom (Sr1) belonging to the Sr sublattice ($\mathbf{a}_1 \mathbf{b}_1 \mathbf{c}_2 \mathbf{q}_2 = \gamma_2 \mathbf{c}_2^*$) and by one (Mn,Co) site (Mn1/Co1) and one O site (O1) belonging to the $(\text{Mn}_{1-x}\text{Co}_x)\text{O}_{3+\delta}$ sublattice ($\mathbf{a}_1 \mathbf{b}_1 \mathbf{c}_1 \mathbf{q}_1 = \gamma_1 \mathbf{c}_1^*$). Occupational and displacive modulations affecting the different atomic domains allow the generation of the structure of $\text{Sr}_{11/8}[\text{Mn}_{5/8}\text{Co}_{3/8}\text{O}_{3+\delta}]$ and $\text{Sr}_{4/3}[\text{Mn}_{2/3}\text{Co}_{1/3}\text{O}_{3+\delta}]$. A displacive modulation is affecting the x and y coordinates of Sr1 (see Fig. SI-2a); this modulation is described by a harmonic function (see Table SI-2). The electron density corresponding to the Mn and Co atoms is plotted in Fig. SI-2b. The same Mn1/Co1 site is describing the positions and displacements of the 2 species; a crenel functions is used to generate Mn and Co position (one crenel is defining the occupation domain of Mn and the other one the domain of Co along x_4) (see Fig. SI-2b); a full occupancy of the octahedral and prismatic environments by Mn and Co atoms respectively has been considered. Finally the O atoms network is depicted using a saw-tooth function (*i.e.* atomic domain defined for a limited interval along x_4 and a linear displacement (see figure SI-2c and table SI-2). Additionally modulation of ADP has been introduced to take into account the variations of environment of Sr atoms.

Crystal I exhibiting a commensurate composite structure, possible 3d sections were tested; the best result is obtained for the section $t_0=1/24$ characterized by the P321 supercell ($a_1, b_1, 3 \times c_1$) space group. To check the validity of our model, the average occupancy of (Mn1,Co1) sites was refined; this parameter does not exhibit significant deviation from the initial value (full occupancy). For the Mo energy, no contrast being observed between Mn and Co the possibility of Co for Mn substitution on the octahedral has not been considered. The final reliability factors and atomic parameters are summarized in Tables SI-1 and SI-2. For the crystal II, owing to the incommensurate character of the modulation, all sections of the (3+1)d structure solution are equivalent and then the analysis of the possible 3d sections is not relevant. As for the crystal I, no evidence for Co vacancy in prismatic

environment is observed. All the information corresponding to this refinement is reported in Tables SI-1 and SI-3.

Super structure analysis of the crystal II

A new structure determination has been performed but in a supercell description ($a_1, b_1, 3 \times c_1$) using the space group P321. The initial structural model can be derived from the previous (3+1)d refinement. The structure is then fully described using 3 strontium sites (Sr1, Sr2, Sr3), 3 manganese sites (Mn1, Mn2 and Mn3), 2 cobalt sites (Co1 and Co2) and 5 oxygen sites (O1, O2, O3, O4 and O5). In this description the A and B atomic columns defined in the figure 6 are built up from (Mn3, Co2, O3, O4) and (Co1, Mn1, Mn2, O1, O2, O5) sites respectively. The structural refinement from this initial model leads to a reliability factor of 5.54%. Considering now the possibility of vacancy in the prismatic environment (i.e. for the Co1 and Co2 sites), a significant decrease of the R factor down to 4.76% is observed. Both Co sites exhibit vacancies but with fully different ratio; Co1 shows about 20% of vacancies and Co2 only 4%. The final composition for this sample is then $Sr_{4/3} Mn_{2/3} Co_{0.301} \square_{0.032} O_3$ in agreement with the formula previously proposed $Sr_{1+y}[(Mn_{2/3}Co_{1/3})_{1-z}\square_z]O_3$ following the oxygen over stoichiometry model. It can be noted in the (3+1)d approach, both A and B columns were described by the same Mn1/Co1 and O1 sites. In this description, the occupancy of the prismatic sites A and B is averaged but the vacancies ratio of the two sites is very different. This effect could be at the origin of the difficulty to evidence the presence of vacancies when the structure is solved using the super space formalism. Results are shown in Tables SI-1 and SI-4.

It should be noted that whatever the approach (classical or superspace), a twin law corresponding to a two-fold axis parallel to c has been introduced for the structure resolution of the crystal I; highly significant it leads to two domains with the 65/35 ratio.

Table SI-1: Details of the refinements for crystals I and II

	Crystal I	Crystal II
Refined composition	$\text{Sr}_{4/3} [(\text{Mn}_{0.602}\text{Co}_{0.064})\text{Co}_{0.301}\square_{0.032}\text{O}_3]$	$\text{Sr}_{4/3}[\text{Mn}_{2/3}\text{Co}_{1/3}\text{O}_3]$
Sublattice 1		
cell parameters (Å)	$a_1 = 9.58782(18)$	$a_1 = 9.5799(6)$
	$b_1 = 9.58723(13)$	$b_1 = 9.5810(3)$
	$c_1 = 2.6019(1)$	$c_1 = 2.5778(5)$
wave vector component	$\gamma_1 = 2/3$	$\gamma_1 = 0.659(1)$
Super space group	R-3m(00 γ_1)s0	R-3m(00 γ_1)s0
Sublattice 2		
cell parameters (Å)	$a_2 = 9.58782(18)$	$a_2 = 9.5799(6)$
	$b_2 = 9.58723(13)$	$b_2 = 9.5810(3)$
	$c_2 = 3.90291(7)$	$c_2 = 3.9105(4)$
wave vector component	$\gamma_2 = 3/2$	$\gamma_2 = 1.517(1)$
Super space group	X-3c1(00 γ_2)000	X-3c1(00 γ_2)000
Rint	0.072	0.0289
Refinement software	Jana2006[3]	Jana2006[3]
Supercell approach:		
Space group	P 3 2 1	
Reliability factor	4.98	
Refinement parameters	62	
Superspace approach:		
Refinement parameters	24	23
Reflections with $I \geq 3\sigma(I)$ / agreement factor (%):		
Main	344 / 5.04	288 / 3.72
1 st order satellites	470 / 6.35	361 / 8.45
2 nd order satellites	353 / 10.98	266 / 20.94
3 rd order satellites	98 / 14.70	193 / 29.05
4 th order satellites	17 / 12.14	

Table SI-2: Atomic parameters for Crystal I in the (3+1)d approach: harmonic function $u_i(\bar{x}_4) = s,n \sin 2\pi n \bar{x}_4 + c,n \cos 2\pi n \bar{x}_4$, crenel function: an occupational domain with a width of Δ along x_4 and centered in x_4^0 , sawtooth function: linear atomic displacement defined by a slop of Δz on a domain with a width of Δ along x_4 and centered in x_4^0

atom	occ	wave	x	y	z	$u_{eq} (\text{\AA}^2)$
Sr1	0.3333		0.3333	0	0.25	0.0072(2)
Position wave	Harmo- nic	s,1	0.01058(4)	0.02116(8)	0	
		c,1	-0.01832(7)	0	0	
		s,2	0.00498(4)	0.00996(7)	0	
		c,2	0.00862(6)	0	0	
Mn1 / Co1	0.1667		0	0	0.5	0.0101(4)
Position wave	Harmo- nic	s,1	0	0	0	
		c,1	0	0	0	
		s,2	0	0	-0.0054(9)	
		c,2	0	0	0	
Occupation wave for Mn1	crenel	$\Delta = 0.3333$				
		$x_4^0 = 0.5$				
Occupation wave for Co1	crenel	$\Delta = 0.1667$				
		$x_4^0 = 0.75$				
O1	0.5		0	0.1568(4)	0	0.012(2)
Positional wave	Harmo- nic	s,1	0	0.0063(16)	0	
		c,1	-0.0107(12)	-0.0054(6)	0	
	saw tooth		0	0	$\Delta z = -0.135(3)$	
		$x_4^0 = 0.75$	$\Delta = 0.5$			

Table SI-3: Atomic parameters for the crystal I in the supercell approach

atoms	occupancy	x	y	z	$u_{eq} (\text{\AA}^2)$
Sr1	1	-0.31220(13)	-0.33617(15)	-0.25045(8)	0.0076(3)
Sr2	1	0	-0.35879(11)	0	0.0045(3)
Sr3	1	0	-0.3257(2)	-0.5	0.0106(4)
Mn1	1	0	0	-0.3354(2)	0.0026(3)
Co1	0.798(9)	0	0	0	0.0091(2)
Mn2	1	0.3333	-0.3333	0.1039(3)	0.0066(4)
Mn3	1	0.3333	-0.3333	-0.5714(3)	0.0073(4)
Co2	0.953(7)	-0.6667	-0.3333	-0.2354(3)	0.0091(2)
O1	1	0	0.1514(10)	-0.5	0.0082(9)
O2	1	0.3459(8)	-0.4827(9)	0.2648(7)	0.0082(9)
O3	1	0.4996(9)	-0.3186(8)	-0.0374(7)	0.0095(17)
O4	1	-0.1615(8)	-0.0060(11)	-0.1973(6)	0.009(2)
O5	1	0.4929(10)	-0.3250(11)	-0.4301(9)	0.025(3)

Table SI-4: Atomic parameters for Crystal II in the (3+1)d approach: harmonic function $u_i(\bar{x}_4) = s,n \sin 2\pi n \bar{x}_4 + c,n \cos 2\pi n \bar{x}_4$, crenel function: an occupational domain with a width of Δ along x_4 and centered in x_4^0 , sawtooth function: linear atomic displacement defined by a slop of Δz on a domain with a width of Δ along x_4 and centered in x_4^0

atom	occ	wave	x	y	z	$u_{eq} (\text{\AA}^2)$
Sr1	0.3333		0.3333	0	0.25	0.0091(3)
Position wave	Harmonic	s,1	0.01050(6)	0.02099(13)	0	
		c,1	-0.0182(2)	0	0	
		s,2	0.00514(5)	0.01028(10)	0	
		c,2	0.00891(8)	0	0	
		S,3	0	0	-0.0021(3)	
		C,3	0	0	0	
Mn1 / Co1	0.1667		0	0	0.5	0.0094(5)
Position wave	Harmonic	s,1	0	0	0	
		c,1	0	0	0	
		s,2	0	0	-0.0067(9)	
		c,2	0	0	0	
Occupation wave for Mn1	crenel	$\Delta = 0.3408$				
		$x_4^0 = 0.5$				
Occupation wave for Co1	crenel	$\Delta = 0.1592$				
		$x_4^0 = 0.75$				
O1	0.5		0	0.1572(5)	0	0.012(2)
Positional wave	Harmonic	s,1	0	0	0	
		c,1	-0.0076(10)	-0.0038(5)	0	
	sawtooth		0	0	$\Delta z = -0.140(3)$	
			$x_4^0 = 0.75$	$\Delta = 0.5$		

Table SI-5: metal–metal distances along c within a Co–Mn chain (\AA); see figure 10 for detailed values in crystal II

	Crystal I		Crystal II
	Chain A	Chain B	Chain A \equiv Chain B
Trimeric "Oh ₂ Tp"			
d Co – Mn	2.626(8)	2.581(8)	$2.567 \leq d \leq 2.608$
d Mn – Mn	2.554(6)	2.570(6)	$2.55 \leq d \leq 2.56$
d Mn – Co	2.626(8)	2.655(8)	$2.567 \leq d \leq 2.608$
tetrameric "Oh ₃ Tp"			
d Co – Mn			$2.607 \leq d \leq 2.608$
d Mn – Mn /			$2.561 \leq d \leq 2.566$
d Mn – Mn			$2.561 \leq d \leq 2.566$

d Mn – Co		$2.607 \leq d \leq 2.608$
-----------	--	---------------------------

Table SI-6: M'–O and M–O distances and Tp height (Å)

	Crystal I		Crystal II
	Chain A	Chain B	Chain A \equiv Chain B
d M – O	3x [1.873(8)] 3x [1.942(6)]	3x [1.895(9)] 3x [1.926(7)] 3x [2.006(7)] 3x [1.83(1)]	3x [1.780(6) \leq d \leq 2.061(6)]
d M' – O	3x [2.160(8)] 3x [2.160(8)]	3x [2.143(9)] 3x [2.162(8)]	3x [1.779(6) \leq d \leq 2.247(8)]
Tp height d O-O	3.063(1)		3x [3.072(1) \leq d \leq 3.074(1)]

References

- [1] Incommensurate Crystallography, Sander van Smaalen, Oxford Science Publications
- [2] Rigaku (2015). CrysAlisPro Software System, Rigaku Oxford Diffraction
- [3] "Crystallographic Computing System JANA2006: General features", V. Petricek, M. Dusek and L. Palatinus, *Z. Kristallogr.*, 2014, 229(5), 345-352. DOI 10.1515/zkri-2014-1737

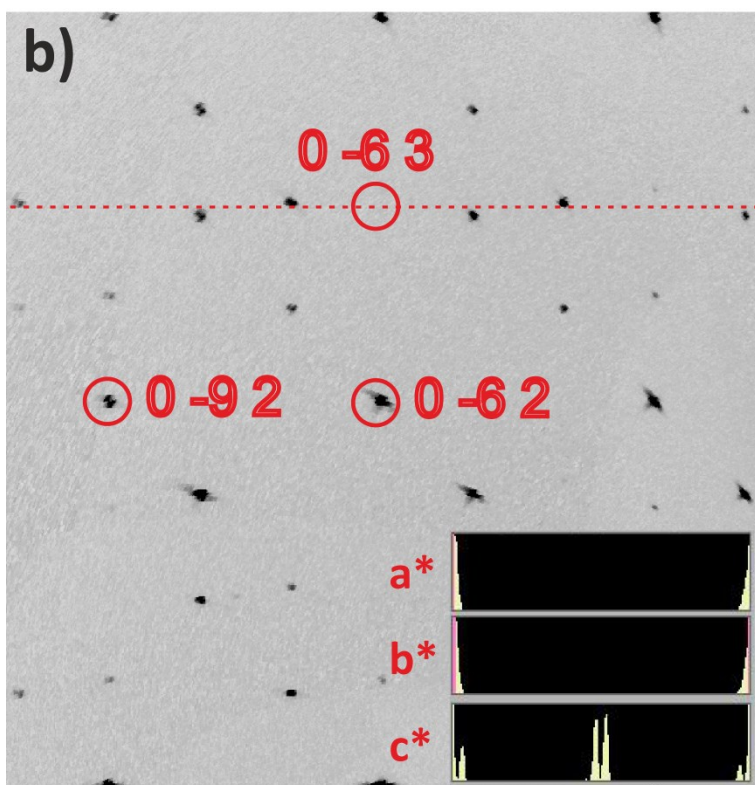
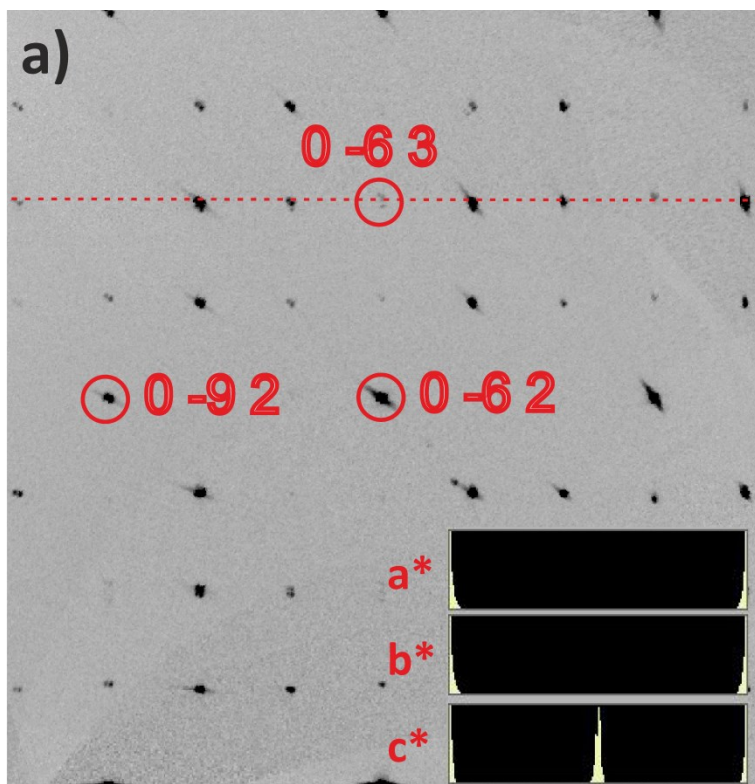


Figure SI-1: $(0kl)^*$ planes reconstructed from experimental frames for the crystals I (a) and II (b). The indexed reflections are belonging to the sub lattice 2. The red dashed line is a guide for the eyes evidencing for the crystal II (b) a misalignment of the diffraction spots related to the aperiodic character of the crystal. Inserts at the bottom of both subfigures are showing along the c^* direction the existence of additional reflections in the vicinity of $\frac{1}{2} c^*$; for b) the observed split is related to the deviation of γ_2 from $3/2$; second order satellites are observed close to 0 and $1 c^*$.

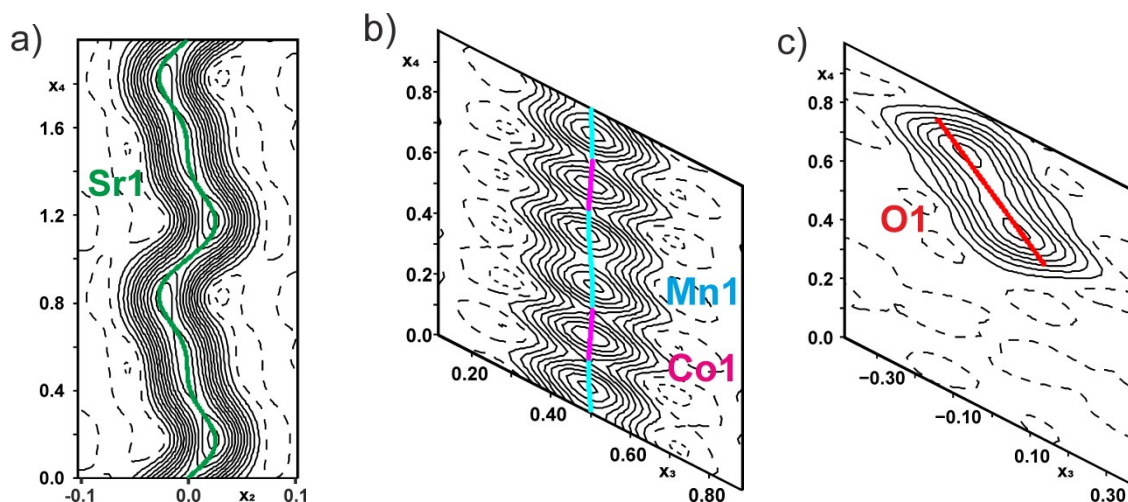


Figure SI-2: de Wolff sections for crystal I (observed Fourier map in the superspace approach): a) $x_2 - x_4$ calculated around the expected position of Sr1 (in the sublattice 2 setting), b) and c) $x_3 - x_4$ calculated around the Mn/Co and O1 positions respectively. The functions refined for each atomic domain are drawn using colored lines or segments.

Estimation of the oxygen content by thermo-gravimetric analysis:

The oxygen content of the samples was determined by thermogravimetric analyses (TGA), using 10% $H_2/90\%$ Ar as a reducing gas at $900^\circ C$ in a Setaram TG92. The oxygen content was determined based on the weight loss and the oxygen content of the residual species (SrO, MnO and Co). The weight loss is the difference between the initial sample mass at room temperature (RT) and the sample mass at $900^\circ C$ (instead of the sample mass at the end of the experiment, at RT). The results are only an estimation and are not rigorously quantitative in nature due to the buoyancy effect, which cannot be precisely taken in account. An example of TGA on the compound $x=3/8$ is given on figure SI-3.

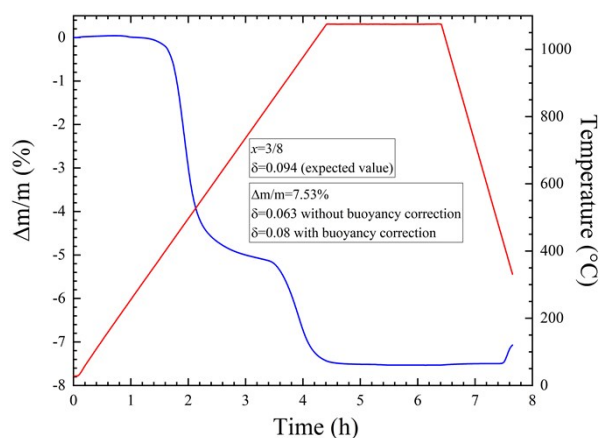


Figure SI-3: Thermo-gravimetric analysis for the compound $x=3/8$ that have an expected over-stoichiometry $\delta=0.094$.